Methane-fed microbial communities enriched from field-grown rice support diverse heterotrophic bacteria

Elena K. Perry[1], Aqib Hasnain[1], Benjamin J. Cole[2], Hans K. Carlson[1], Adam M. Deutschbauer[1], Dawn Chiniquy[1]*

[1]Environmental Genomics and Systems Biology Division, Lawrence Berkeley National Laboratory, Berkeley, CA, USA

[2]DOE Joint Genome Institute, Lawrence Berkeley National Laboratory, Berkeley, CA, USA

*Correspondence: dmchiniquy@lbl.gov

Abstract

Rice paddies naturally host significant populations of methanotrophs, due to the production of methane in flooded soils. However, relatively little is known about how the activity of these bacteria impacts the structure of the broader microbial community in this important agricultural environment. To address this question, we passaged 51 microbial aerobic enrichment cultures from rice rhizosphere, root, and stem samples in a chemically-defined medium with methane as sole electron donor. We profiled the cultures over time by 16S rDNA amplicon sequencing and sequenced the genomes of 34 isolates from the enrichments to gain functional insights. Notably, taxa whose relative abundance increased during community growth on methane represented more than a dozen families, many of which are not known to utilize methane or other one-carbon substrates. Despite the selective pressure imposed by the culture condition, the final community structures were taxonomically varied rather than converging to a common composition, and genomic analysis of the sequenced isolates revealed considerable variation in likely carbon source utilization repertoires. Taken together, these findings support the view that methanotrophy represents a key link in the microbial food web of rice fields, with the potential for downstream effects on the abundance and activity of a wide range of community members.

Introduction

Microbes that oxidize one-carbon compounds, such as methane and methanol, play a key role in global nutrient cycles. In particular, aerobic methanotrophs in the phylum Pseudomonadota are the most widespread functional guild contributing to microbial methane oxidation. Aerobic methanotrophs are classically divided into two major groups, Type I (Gammaproteobacteria) and Type II (Alphaproteobacteria); Type I methanotrophs use the ribulose monophosphate (RuMP) pathway for carbon assimilation into biomass, while Type II use the serine pathway. Because these bacteria can use methane as a sole carbon and energy source, they are found in a variety of environments where methane is abundant, such as wetlands, freshwater lake sediments, and landfill cover soils (1). Besides contributing to carbon cycling via methane oxidation, methanotrophs may also play an important role in the global nitrogen cycle, as many proteobacterial methanotrophs are capable of nitrogen fixation (2). Conversely, methanotrophs have also been shown to stimulate the activity of denitrifying bacteria (3, 4).

Consistent with the latter observation, it is thought that methanotrophs often interact metabolically with other members of their native microbial communities (5). Methanotrophs are notoriously difficult to isolate (6), and culturing methanotrophs in the presence of other heterotrophic bacteria frequently increases methane oxidation rates and overall biomass yields (7, 8). Such partnerships may benefit the methanotrophs by preventing the accumulation of inhibitory metabolic byproducts or providing essential vitamins (7, 9). Methanotrophs can in turn provide benefits to their neighbors. Studies using stable-isotope probing (SIP) have demonstrated that carbon derived from methane by methanotrophs in a variety of environments can end up in the biomass of diverse other organisms (10–15). Thus, methanotrophs contribute to local microbial food webs by transforming methane into other, more bioavailable carbon sources.

48 While the existence of metabolic exchanges between methanotrophs and other bacteria is
49 well-established, relatively little is known about how methanotrophs influence the microbial
50 communities of methane-rich wetland environments, including rice paddies (16). Recently,
51 methanotrophs have been shown to stimulate both nitrogen fixation and denitrification in rice
52 paddies, depending on the environmental conditions (12, 17), but the full range of their impact on
53 the rice microbiome remains unclear. Given the roles of methanotrophs in both carbon and nitrogen
54 cycling, an improved understanding of their ecological influence in rice paddies could have
55 significant implications for improving the productivity and sustainability of rice cultivation. This
56 issue is of global importance since rice is one of the world's most widely-consumed staple crops
57 (18). The most concrete evidence that specific taxa might preferentially benefit from methane-
58 derived carbon in rice fields has come from DNA-SIP studies on microcosms of paddy soils or
59 rice roots (10, 12). In these studies, the bacteria that incorporated the ^{13}C label mainly belonged to
60 the Alphaproteobacteria and Betaproteobacteria, although the results varied at lower taxonomic
61 levels. However, the sensitivity of DNA-SIP is limited and the results can be significantly affected
62 by experimental parameters such as incubation time (19), thus motivating the use of
63 complementary approaches to determine the range of microbial taxa that may profit from
64 methanotrophic activity in rice fields.

65 Here, we performed 16S rDNA gene-based profiling on methane-fed enrichment cultures,
66 complemented by whole-genome sequencing of strains isolated from the enrichments, to gain new
67 insights into how methanotrophs from rice paddies influence their native communities.
68 Specifically, we addressed the following questions: 1) What is the taxonomic diversity of rice-
69 associated bacteria that can be supported by methane-derived carbon? 2) To what extent is the
70 community composition of methane-fed enrichment cultures affected by external variables such

71 as the part of the rice plant used for the inoculum? 3) Is the impact of methanotrophs on the rice
72 microbiome predictable, as indicated by recurring community assembly patterns (if any) during
73 growth on methane as the sole exogenous carbon source? 4) What carbon sources are the most
74 likely drivers of non-methanotrophic growth in methane-fed, methanotroph-anchored
75 communities?

76 **Results**

77 *Methane-fed enrichment cultures maintained high alpha diversity*

78 We established 51 enrichment cultures in chemically-defined media with methane as the
79 sole electron donor and oxygen as the major electron acceptor, inoculated with rice rhizosphere,
80 root, and stem samples collected from two field locations in California, as described in Materials
81 and Methods. The cultures were sampled weekly over 12 weeks for 16S amplicon-based profiling
82 of community composition, resulting in a total of 534 sequenced samples (excluding those that
83 failed to meet our threshold for minimum reads; see Materials and Methods); the complete ASV
84 abundance table and sample metadata are available in Tables S1 and S2, respectively. At the final
85 time point, 16 families belonging to three phyla (Pseudomonadota, Bacteroidota, and
86 Verrucomicrobiota) achieved a relative abundance of >10% in at least two enrichments (Fig. 1A).
87 Two additional higher-level taxonomic groups, consisting of ASVs that could not be classified
88 beyond the order Rhizobiales or the domain Bacteria, met the same criteria for abundance and
89 prevalence. By far the most prominent families across the final enrichment communities, when
90 considering both prevalence and relative abundance, were Comamonadaceae (>10% in 33/51
91 enrichments, mean relative abundance 16.3%) and Methylocystaceae (>10% in 29/51 enrichments,
92 mean relative abundance 22.4%). Comamonadaceae does not contain any known methanotrophs,
93 but Methylocystaceae represents the Type II methanotrophs. Type I methanotrophs, represented

by the family Methylococcaceae, were less prevalent in the final enrichments (>10% in 4/51 enrichments).

Interestingly, while all of the final enrichment communities contained a detectable level of at least one putative methanotroph ASV classified as Methylocystaceae or Methylococcaceae, methanotrophs were not always the most abundant community members. Methanotrophs represented the majority of reads in just eight out of the 51 final communities. In 16 out of the 51 enrichments (nearly 1/3) the final total methanotroph relative abundance was <10%, and the lowest final total methanotroph relative abundance was just 0.2%. Inspecting the relative abundances of putative methanotroph ASVs over time revealed that in many of the enrichments, methanotroph abundances fluctuated or dropped after reaching a peak prior to the final time point, rather than steadily increasing over time—especially for many of the Type I methanotrophs (Fig. 1B). Additionally, in most of the enrichments only one or two methanotroph ASVs were abundant at any given time (Fig. 1B-C). By contrast, individual enrichments supported up to 80 non-methanotroph ASVs (with a median of 39) at the final time point (Fig. 1C).

We also assessed how overall alpha diversity was affected by time, sample type, and initial inoculum dilution. For rhizosphere and root enrichments, the number of ASVs observed per enrichment initially dropped noticeably compared to the inoculum, but subsequently fluctuated around the value reached by the end of week one, rather than continuing to decline, despite the 1:10 dilution transfers that were performed after week four and week eight (Fig. 1D). For stem enrichments, the number of observed ASVs dropped only slightly in the first week, and fluctuated around the original value thereafter (Fig. 1D). Community evenness followed generally similar patterns over time for the different sample types (Fig. 1E). At the final time point, the number of observed ASVs was significantly lower for stem enrichments compared to rhizosphere and root

117 enrichments, but did not differ between the latter two groups (Fig. 1F). Initial inoculum dilution
118 had no statistically significant effect on the final number of observed ASVs (Fig. 1G).

119 *Beta diversity arose primarily from individual variation between enrichments rather than external*
120 *variables*

121 The taxa bar plots for the final time point indicated considerable variability in community
122 composition across the enrichments (Fig. 1A). We therefore performed additional analyses to
123 assess the impact of three external variables on beta diversity: time since inoculation, field site of
124 origin, and original sample type. PERMANOVA analysis indicated that time had a significant
125 effect on beta diversity regardless of whether ASV abundances and phylogenetic relationships
126 were accounted for (p = 0.001 for both Jaccard and weighted UniFrac distances) (Table 1).
127 However, the effect was relatively small (R^2 = 0.04 and 0.08 for Jaccard and weighted UniFrac
128 distances, respectively), and the respective PCoA plots suggested that the effect was not
129 particularly consistent over time or across different enrichments (Fig. 2A). Indeed, the time to
130 reach a stable community composition varied across the enrichments, with some appearing to
131 largely stabilize following the first 1:10 dilution transfer after week four; some experiencing
132 another dramatic shift following the second 1:10 dilution transfer after week eight; and a few
133 appearing to undergo a more or less continuous shift starting after the first transfer and continuing
134 to the end of the experiment (Fig. S1). Additionally, PERMDISP analysis indicated that the sample
135 dispersions differed significantly across different time points (p = 0.001 for both Jaccard and
136 weighted UniFrac distances) (Table 1), which can cause a significant PERMANOVA result even
137 if there is no difference in the group centroids.

138 The field site of origin (Biggs versus Staten Island) also had a statistically significant effect
139 on community composition (PERMANOVA p = 0.001 for both Jaccard and weighted UniFrac

140 distances, permuting only within each time point given the significant effect of time) (Table 1).
141 However, while the PCoA plot based on Jaccard distances revealed an almost perfect separation
142 between enrichments from the two fields, this was not evident with weighted UniFrac distances
143 (Fig. 2B), and the overall effect of field site was again quite small in both cases (R^2 = 0.05 and
144 0.03 for Jaccard and weighted UniFrac distances, respectively). Original sample type (rhizosphere,
145 root, or stem) also had a significant effect on community composition (PERMANOVA p = 0.001
146 for both Jaccard and weighted UniFrac distances, permuting only within each time point), with
147 slightly larger effect sizes (R^2 = 0.07 and 0.13 for Jaccard and weighted UniFrac distances,
148 respectively). Indeed, while the PCoA plots suggested a high degree of overlap among rhizosphere
149 and root enrichments, the stem enrichments clustered somewhat separately based on both Jaccard
150 and weighted UniFrac distances (Fig. 2C). However, PERMDISP indicated that as with the effect
151 of time, sample dispersions also differed for the two field sites and across the different sample
152 types (p = 0.001 for both Jaccard and weighted UniFrac distances) (Table 1).

153 In contrast to the relatively small effects of the above variables, by far the greatest
154 proportion of the beta diversity was explained by individual enrichment identity, i.e. the unique
155 combination of field site, sample type, replicate, and dilution (PERMANOVA p = 0.001, R^2 = 0.44
156 for weighted UniFrac) (Table 1). The marginal effects of replicate and dilution were very small
157 (R^2 = 0.01 and 0.02 respectively), although still statistically significant (p = 0.001) (Table 1). We
158 therefore also asked whether enrichments derived from the same original sample but with different
159 inoculum dilutions ("within sample") ended up more similar to each other at the final time point
160 than enrichments derived from different original samples ("between sample"). In the case of
161 Jaccard distances (which take into account only the presence/absence of each ASV), there was a
162 statistically significant difference for the "within sample" versus "between sample" comparison

163 (Fig. 2D). This intuitively makes sense as enrichments derived from the same original sample
164 would be expected to share a higher proportion of ASVs, given the lack of opportunities for
165 dispersal between the enrichments over time. Notably, however, based on the weighted UniFrac
166 metric, which provides an arguably better representation of overall differences in community
167 structure, there was no statistically significant difference for "within sample" versus "between
168 sample" distances.

169 *Stochastic processes dominated the enrichment community assembly*

170 Given the high degree of variability in final community composition, even across
171 individual enrichments derived from the same original sample, we hypothesized that stochastic
172 processes had contributed significantly to community assembly in the enrichments. We therefore
173 sought to quantitatively infer the contribution of stochastic versus deterministic ecological
174 processes (i.e. drift versus selection), using two related statistical methods known as QPEN
175 ("Quantifying assembly Processes based on Entire-community Null model analysis") and iCAMP
176 ("infer Community Assembly Mechanisms by Phylogenetic-bin-based null model analysis") (20–
177 22). Both approaches are founded on the observation that more closely related species tend to
178 occupy more similar niches; thus, if the abundance-weighted phylogenetic relationships between
179 two communities' members are on average significantly closer than expected by chance given the
180 full set of taxa observed across all communities, this suggests that deterministic selection is at
181 work in similar environments. Consistent with our hypothesis, QPEN suggested that ecological
182 drift was the dominant process for 75% of all pairwise comparisons among the final enrichment
183 communities, while homogenous selection was the dominant ecological process for just 5%.
184 Similarly, iCAMP indicated that drift was the dominant process for the majority of phylogenetic

185 bins in 70% of the pairwise comparisons, while dispersal limitation and homogenous selection
186 were dominant in 8% and 5% of the comparisons respectively.

187 As an orthogonal approach to assess the potential contribution of deterministic forces to
188 the assembly of the enrichment communities, we performed consensus clustering analysis on the
189 final communities after collapsing the taxonomy abundance table to the family level. Consensus
190 clustering is a method of estimating how many subclasses (in this case, types of community
191 structures) are present in a dataset (23), and has previously been used to infer whether deterministic
192 forces contributed to variation across different enrichment communities (24). Specifically, if the
193 number of inferred community types is much less than the number of samples, this would suggest
194 some degree of determinism (non-randomness) in the community assembly process. Inspection of
195 the delta area plot (in which lower values represent lesser gains in cluster stability with increasing
196 *k*), as well as the cumulative distribution functions and heatmaps of the consensus matrices for
197 different *k*'s (numbers of clusters), suggested that the optimal number of clusters was 9 (Fig. 3A-
198 C, Fig. S2). However, clusters 5, 6, 7, and 9 were represented by only a single enrichment each.
199 Organizing the taxonomy abundance bar plots by cluster identity suggested that cluster 1 (the
200 largest cluster) was driven by a relatively high abundance of Methylocystaceae, whereas cluster 2
201 (the second-largest cluster) was driven by a high abundance of Comamonadaceae paired with a
202 lower abundance of Methylocystaceae (Fig. 3D). Cluster 3 was appeared to be driven by a high
203 abundance of ASVs that could not be classified beyond the domain Bacteria, cluster 4 was driven
204 by a high abundance of Methylococcaceae, and cluster 8 was driven by a high abundance of
205 Chromobacteriaceae. The samples in the singleton clusters did not fall into any of these categories.

206 Taken together, these results suggest that despite the uniform culture conditions and
207 theoretically strong selective force imposed by the use of minimal media with methane as the only

208 added electron donor, stochastic processes (such as chance colonization—i.e. which strains were
209 present at time zero—and random extinction) were important drivers of community assembly in
210 our enrichments. Accordingly, even though certain types of community structures were more
211 prevalent than others among the final enrichments (as revealed by the consensus clustering
212 analysis), unpredictable and unique community structures also emerged.

213 *Putative parasitic bacteria belonging to the Candidate Phylum Radiation transiently bloomed in*
214 *multiple independent enrichments*

215 We were intrigued by the observation that ASVs that could not be classified beyond the
216 domain Bacteria were abundant in several of the enrichments. This was particularly striking in the
217 case of the final timepoint of the Staten Island root 2 10^{-2} enrichment, where the relative abundance
218 of a single unclassified bacterial sequence, ASV607, was 40.9%. Besides ASV607, five other
219 unclassified bacterial ASVs appeared at a relative abundance of >5% at least three times in our
220 enrichment time course dataset: ASV611, ASV616, ASV684, ASV697, and ASV891 (Fig. 4A). To
221 gain insight into the possible nature of these taxa, we used BLAST to search the respective ASV
222 sequences against the NCBI core nucleotide database (Table S3). For ASV697, the best named hit
223 was uncultured member of Chlamydiota detected in Chinese rice paddy soil, while for ASV684,
224 the best named hit was an uncultured member of Lentisphaerota detected in lake sediment (also
225 located in China), another environmental source of methane. For ASV616, there was no named hit
226 with coverage >50%, but the top overall hits were from environments such as subsurface water, a
227 sewage stabilization pond, and floodplain soil. For all three of the remaining sequences, the top
228 named hits belonged to the members of the Candidate Phylum Radiation (CPR)—specifically, the
229 candidate phyla Altimarinota (a.k.a. Gracilibacteria; ASV607 and ASV611) and
230 Peregrinibacteriota (ASV891). Notably, the top overall hit for ASV891 was a 100% match to an

231 unclassified 16S sequence from water that had been used to rinse rice grains; the second-best
232 overall hit for ASV607 was a 97.83% match to an unclassified 16S sequence from the "heavy"
233 isotopic fraction of activated sludge that had been incubated with ^{13}C-labeled methane; and the top
234 overall hits for ASV611 included sequences from lake sediment and a wetland. Taken together,
235 these results suggest that bacteria closely related to the unclassified sequences in our enrichments
236 might commonly occur in environments where methane is abundant.

237 Given that ASV607 was the most prevalent and abundant unclassified ASV in our
238 enrichments (Fig. 4A), we focused on this taxon for further analysis. Members of the CPR, to
239 which ASV607 putatively belongs, are mostly uncultivated but are thought to primarily be ultra-
240 small (~200-500 nm diameter) episymbiotic parasites of other bacteria (25, 26). To determine
241 whether such bacteria were present in a sample containing ASV607, we performed scanning
242 electron microscopy (SEM) on the Staten Island root 2 10^{-2} enrichment after regrowing it from a
243 frozen glycerol stock under the same conditions as the original enrichment. Strikingly, we found
244 multiple examples of such a bacterium in this culture: small (~340 nm diameter) cocci or
245 diplococci that in all cases (n = 4) appeared to be directly attached to a larger host (Fig. 4B).
246 Although we cannot be sure that these bacteria represent ASV607, these observations lend
247 credence to the possibility that ASV607 is an episymbiont, similar to other studied members of the
248 CPR.

249 Finally, we attempted to identify of the potential host(s) of ASV607 by looking for other
250 ASVs whose abundances were correlated with this taxon. Since ASV607 might by chance not
251 occur in every enrichment where its host was present, we first subsetted our enrichment time course
252 dataset to only the enrichments where ASV607 was detected at least once. We then used two
253 complementary methods of correlation analysis: SparCC, which was designed to handle some of

254 the challenging characteristics of microbiome data (e.g. compositionality and sparsity) (27), and
255 Pearson correlation, the method with the highest sensitivity for detecting parasitic interactions in
256 a prior study based on simulated data (28). Importantly, the latter study also demonstrated that
257 parasitic interactions between two taxa usually present as positive correlations (i.e. co-occurrence)
258 rather than negative correlations in microbial abundance data (28). Only two ASVs were
259 significantly positively correlated with ASV607 according to both methods: ASV7 (classified as
260 Methylophilaceae) and ASV441 (classified as Spartobacteria). When we highlighted the
261 abundances of these ASVs in the enrichments where ASV607 occurred, it became clear that
262 ASV607 occurred at relatively high abundances in multiple enrichments where ASV441 was
263 consistently below detection (Fig. 4C). By contrast, ASV7 was detected at least once in all of the
264 enrichments where ASV607 was abundant, and at many timepoints these two taxa co-occurred
265 with similar relative abundances (Fig. 4C). Thus, although we currently cannot rule out the
266 possibility that ASV441 (or other taxa) could be a host for ASV607, ASV7 (Methylophilaceae)
267 appears to be the most likely candidate for the primary host.

268 *Strains isolated from the enrichments possess variable catabolic repertoires*

269 Given that the enrichment cultures were fed only with methane, the abundance and
270 diversity of non-methanotrophic strains raised the question of what carbon sources could be
271 supporting their growth. Methanotrophic activity has been shown to contribute to the pool of
272 organic acids in rice paddy soils (12). Additionally, it has been previously reported that some
273 methanotrophs can cross-feed methanol (the first product of methane oxidation) to non-
274 methanotrophic methylotrophs (29). We therefore investigated whether organic acids and/or
275 methanol could plausibly support the growth of members of the enrichment communities.

To do so, we isolated a total of 65 strains from the enrichments (Table S4). Of these isolates, three are methanotrophs (*Methylosinus* DMC42, *Methylosinus* DMC45, and *Methylocystis* DMC101), while the rest are non-methane-utilizing heterotrophs. The isolates represent 12 of the 16 families that had reached a final relative abundance of >10% in at least two enrichments (missing representatives only for Verrucomicrobiaceae, Methylococcaceae, Bradyrhizobiaceae, and Prolixibacteraceae). Three isolates belonging to the genus *Methyloraptor*, in the family Ancalomicrobiaceae, matched a similarly prevalent and abundant ASV that had been classified only to order level as Rhizobiales. We also obtained isolates for several other families that were less prevalent and/or abundant in the final enrichments, including Moraxellaceae, Sphingomonadaceae, Xanthobacteraceae, Caulobacteraceae, Devosiaceae, Microbacteriaceae, Sphaerotilaceae, and additional members of Rhizobiaceae (one of which had dominated a Biggs stem enrichment).

To obtain strain-level insights into the potential catabolic capabilities of the enrichment community members, we generated draft genome assemblies for a diverse selection of isolates representing most of the families in our collection. We then assessed the non-methanotrophic isolates' genomic potential for the consumption of 62 common carbon sources, using the program GapMind (30). We considered a strain likely to be able to use a carbon source if GapMind identified a complete pathway with only high-confidence hits, and a "maybe" if GapMind identified a complete pathway but at least one step was at best a medium-confidence hit. Strains were considered unlikely to be able to use a carbon source if any of the best hits in the respective pathway were low-confidence, i.e. "gaps." This analysis revealed that nearly all of the sequenced isolates are likely to be able to use fumarate as a carbon source, and most of the isolates (with the exception of members of Methylophilaceae and *Cloacibacterium*) are also likely to be able to use

299 multiple other organic acids, such as succinate, malate, and acetate (Fig. 5). By comparison, the
300 capacity to utilize sugar-related compounds and amino acids as carbon sources appeared to be less
301 widespread.

302 We also assessed whether the non-methanotrophic isolates could potentially utilize
303 methanol, which is not included in GapMind. To do so, we searched the genomes for homologs of
304 the four known types of methanol dehydrogenases (MxaF, XoxF, Mdh2, and NAD-dependent Mdh)
305 (Fig. 6A). For strains that possessed a putative homolog of at least one of these genes, we also
306 looked for homologs of the genes needed for the ribulose monophosphate (RuMP) cycle, the serine
307 cycle, and the Calvin-Benson cycle, which are the three known pathways for assimilation of C1
308 units by methylotrophic bacteria (31) (Fig. 6B). The results were mostly consistent with what has
309 been reported for the respective taxonomic groups: members of *Methylovorus*, *Methylophilus*,
310 *Methylobacterium*, *Methyloraptor, Oharaeibacter*, and *Xanthobacter* are all known methylotrophs,
311 and all sequenced isolates from these genera possessed both MxaF and XoxF, as well as a complete
312 C1 assimilation pathway. However, one isolate from a genus not known to be methylotrophic also
313 showed possible genomic capacity for methylotrophy: *Pinisolibacter* sp. DMC19 possesses a
314 homolog of XoxF as well as a complete Calvin-Benson cycle. Another *Pinisolibacter* isolate also
315 possesses XoxF, but appears to be missing a key enzyme in the Calvin-Benson cycle
316 (glyceraldehyde-3-phosphate dehydrogenase), while *Oryzibacter oryziterrae* DMC98 possesses
317 XoxF along with a near-complete serine cycle, but appears to be missing phosphoenolpyruvate
318 carboxylase. A few other isolates from genera not typically known to consume methanol contained
319 putative homologs of XoxF, Mdh2, and/or NAD-dependent Mdh, but lacked multiple steps in each
320 of the C1 assimilation pathways, suggesting that they are unlikely to use methanol as a carbon
321 source.

322 **Discussion**

323 In this study, we utilized methane-fed enrichment cultures to determine which bacterial
324 members of the rice microbiota can be supported by methane-derived carbon, revealing
325 considerable taxonomic diversity among the potential beneficiaries of methanotrophic activity. We
326 found that the composition of rice-derived, methane-supported microbial communities is
327 significantly affected by the type of plant part used as the inoculum (with stem enrichments
328 exhibiting lower alpha diversity than root and rhizosphere enrichments), but is less affected by
329 field site. While many of our enrichments had a high abundance of type II methanotrophs and/or
330 members of Comamonadaceae, a variety of overall community structures emerged, suggested a
331 limited contribution of deterministic forces to community assembly during growth on methane.
332 Finally, genomic analysis indicated that organic acids and methanol are likely carbon sources that
333 may support the growth of many non-methanotrophs in methane-fed communities. Taken together,
334 these results shed new light on the contribution of methanotrophs to the rice microbiome.

335 The diversity of non-methanotrophic taxa that were enriched alongside methanotrophs in
336 our cultures, representing at least 14 families, greatly expands the knowledge of which taxa may
337 benefit from methanotrophic activity in rice paddies. In prior DNA-SIP studies where rice roots or
338 paddy soils were incubated with isotopically-labeled methane, relatively few taxa were identified
339 (10–12), possibly due to the limited sensitivity of this technique and the presence of alternative
340 carbon sources in those experimental setups. In our enrichments, as in the DNA-SIP studies, some
341 carbon from the soil or plant material would have been present at the start of the experiment, but
342 any such nutrients would have then been diluted by the two sequential transfers, if not already fully
343 consumed in the first few weeks of incubation. We cannot rule out that nutrients may also have
344 been released by cell lysis over the course of our experiment, potentially supporting some of the

345 taxa that only persisted at a very low relative abundance in the enrichments. Nevertheless, with
346 the possible exception of a few enrichments where the final abundance of putative methanotrophs
347 appeared to be extremely low (which may have occurred due to stochastic extinction), taxa that
348 were abundant at the final timepoint of our enrichments were likely primarily supported by
349 methane-derived carbon. Among the non-methanotrophic taxonomic groups that were particularly
350 prevalent and/or abundant in our enrichments, Comamonadaceae, Methylophilaceae, Rhizobiales,
351 and Sphingomonadales have also been labeled with methane-derived carbon in DNA-SIP studies
352 (10, 12), providing further evidence that these taxa genuinely benefit from methanotrophic activity
353 in rice fields.

354 The heterogeneity of our enrichments indicated a significant contribution of stochastic
355 ecological forces to community assembly during growth under methane. While this may in part
356 have been driven by the particulars of our experimental setup (e.g., the use of a dilution series, and
357 the relatively long four-week incubation time between transfers), the variety of observed
358 community structures, together with the diversity of the enriched taxa, suggests that the impact of
359 altering methanotrophic activity in rice microbiomes might not be easily predicted. That being said,
360 our enrichments also bore some taxonomic resemblance to previous studies on methane-supported
361 microbial communities from other environments. For example, *Methylophilus*, *Pseudomonas*, and
362 *Flavobacterium*, three prominent genera in our enrichments, were also prevalent in methane-fed
363 enrichments from lake sediment (32, 33). Moreover, a study on naturally-occurring methane-
364 supported biofilms in a mineral spring cave reported the presence of Flavobacteriales,
365 Verrucomicrobia, Rhizobiales, Sphingomonadales, Pseudomonadales, and Xanthomonodales,
366 among other non-methanotrophic taxa (34), all of which were abundant in at least two of our
367 enrichments. Thus, it appears that the assembly of methane-supported communities is not entirely

368 random, and many of the taxonomic groups in our enrichments may be associated with
369 methanotrophs not only in rice paddies, but also more broadly.

370 Another notable finding was the unexpected prevalence of CPR bacteria in our enrichments.
371 To our knowledge, this phenomenon has not previously been reported in a methane-supported
372 microbial ecosystem. However, many of the closest sequenced relatives for the putative CPR
373 bacteria in our enrichments were also derived from environments where methane is abundant,
374 indicating that our detection of CPR members in methanotrophic communities is not an anomaly.
375 Given that the DNA of one such organism was labeled with methane-derived carbon in a DNA-
376 SIP study (see Table 2), some of these bacteria may in fact benefit from the activity of
377 methanotrophs. This interpretation is further supported by the positive correlation between
378 ASV607 (a putative CPR member) and ASV7 (a member of the methylotrophic family
379 *Methylophilaceae*) in our enrichments. Notably, standard 16S primer pairs are a poor match for
380 many CPR members (35). Thus, these organisms may be even more prevalent and abundant in rice
381 microbiomes and other methane-supported microbial communities than is reflected in currently
382 available data. Detailed studies on CPR bacteria are unfortunately challenging due to the difficulty
383 of isolating these organisms. Nevertheless, future attempts to confirm the identity of the host(s)
384 for rice-associated CPR bacteria, and to ascertain the nature of the host-epibiont relationship (i.e.,
385 parasitic, predatory, or commensal), may help improve the understanding of rice microbiome
386 dynamics.

387 Finally, regarding the question of how non-methanotrophic growth is supported in
388 methane-fed communities, the prevalence of pathways for organic acid catabolism in isolates from
389 our enrichments suggests that organic acids may be a key class of cross-fed metabolites, consistent
390 with prior evidence that methanotrophs contribute to organic acid production in paddy soils (12).

391 Whether this contribution is primarily direct or indirect remains unclear, but certain type I and type
392 II methanotrophs have been shown to excrete organic acids in pure cultures during growth on
393 methane under low oxygen conditions (36–38). Additionally, the abundance of several
394 methylotrophic taxa in our enrichments suggests that methanol may also have been cross-fed from
395 methanotrophs, as has been previously demonstrated in pairwise co-cultures of a methanotroph
396 and a methylotroph (29). However, organic acids and methanol may not be the only cross-fed
397 carbon sources in methanotroph-supported communities. Several taxa enriched in our cultures
398 belong to the phylum Bacteroidota, members of which are best known for their ability to degrade
399 complex carbohydrates (39). Consequently, it has previously been suggested that Bacteroidota
400 members that frequently co-occur with methanotrophs (e.g., *Flavobacterium* species) may be
401 supported by extracellular polysaccharides produced by other community members, though direct
402 evidence of such interactions is still lacking (5). These taxa proved difficult to isolate from our
403 enrichments, and thus we only have one representative genome sequence so far, from a strain of
404 *Cloacibacterium*. Potentially consistent with the extracellular polysaccharide hypothesis, this
405 strain does not possess high-confidence pathways for the usage of either organic acids or methanol,
406 suggesting that it may indeed have been supported by other compounds in the enrichment cultures.
407 While beyond the scope of the current study, future work will be directed at more precisely
408 identifying the carbon sources exchanged among members of methanotroph-supported microbial
409 communities.

410 In summary, our findings suggest that methanotrophs may help support a wide range of
411 heterotrophic bacteria in the microbial ecosystem of rice paddies. Furthermore, our collection of
412 65 taxonomically-diverse isolates, more than half of which have draft genomes, represents a
413 valuable resource for future mechanistic studies on how rice-associated methanotrophs interact

414 with their native neighbors. Given the recent evidence that methanotrophs affect not only carbon
415 cycling but also nitrogen cycling in rice paddies (12, 17), it will be worthwhile to continue gaining
416 a deeper understanding of how methanotrophic bacteria influence the structure and function of the
417 rice microbiome under different conditions, so as to ensure the long-term sustainability and
418 productivity of this globally-important staple crop.

419 **Acknowledgments**

420 This work was funded by the Laboratory Directed Research & Development program
421 (award 23-071) at Lawrence Berkeley National Laboratory. We thank the Sundaresan and
422 Schuppenhauer labs for providing the field-grown rice samples, Deepika Awasthi for assistance
423 with establishing a methane gassing station, Morgan Price for assistance with data processing, and
424 Misun Kang and the staff at the University of California Berkeley Electron Microscope Laboratory
425 for advice and assistance with electron microscopy sample preparation and imaging.

426 **Materials and Methods**

427 *Time course of methane-fed enrichment cultures*

428 Six rice plants were collected from two fields (three plants per field), located in Biggs,
429 California (39.4643, -121.7340) and Staten Island, California (38.1235, -121.5490), in the summer
430 of 2022. The Biggs samples were collected in late July, and the Staten Island samples were
431 collected in late August. Each plant was collected from a different area of the respective field and
432 had the entire root structure dug up with the attached soil. The collected plants were placed in
433 individual clean zipper-top plastic bags in 5-gallon buckets and transported back to the laboratory.
434 The protocol for establishing methane-fed cultures from the rhizosphere was based on previous
435 work (40), with modifications made to include the root and stem. For each plant, after removing
436 soil not tightly bound to roots, a portion of the roots was dissected and placed in a 15 mL conical

437 tube containing 10 mL of dilute nitrate mineral salts (dNMS) media, made according to the recipe
438 of (40) except that the vitamin solution was procured from the American Type Culture Collection
439 (catalog no. MD-VS). The roots were vigorously vortexed to generate the rhizosphere samples.
440 Then, a portion of the roots was ground in 1 mL dNMS for 45 s using a sterilized stainless-steel
441 grinding jar (Qiagen, catalog no. 69985) in a Qiagen TissueLyser II. Stem samples were processed
442 in a similar manner. 0.5 mL of the homogenized samples, representing the week 0 time point, was
443 spun down at 4000 rpm for 20 min in a tabletop centrifuge, and the pellets were stored at -20°C
444 until DNA extraction. The remainder of each sample was diluted 10^{-2}, 10^{-3}, and 10^{-4} in dNMS
445 (Staten Island stem samples were only diluted up to 10^{-3}), and 0.5 mL of the resulting suspensions
446 was injected into sealed, autoclaved Balch tubes containing 5 mL of dNMS. Approximately 5 mL
447 of the headspace was removed by syringe and replaced with 5 mL of methane to create a 20%
448 methane headspace. The cultures were incubated upright with shaking at 24°C. Every seven days,
449 0.5 mL was collected from each culture and pelleted for later DNA extraction as above.
450 Additionally, 70 µL of each culture was used to make a frozen stock in 15% glycerol, stored at -
451 80°C. At the same time, 5 mL of headspace was withdrawn and replaced with another 5 mL of
452 methane. Every four weeks, 0.5 mL of each culture was transferred to a new Balch tube containing
453 5 mL of fresh dNMS. The experiment was terminated after a total of 12 weeks.

454 *16S rDNA amplicon sequencing*

455 Genomic DNA was extracted from pelleted samples using the Qiagen DNeasy Blood &
456 Tissue kit (catalog no. 69506), following the manufacturer's protocol for Gram-positive bacteria.
457 The extracted DNA was PCR amplified using dual-index 16S V4-V5 primers (515F/926R) (41).
458 A peptide nucleic acid (PNA) PCR clamp was used to block the amplification of plastid and
459 mitochondrial DNA (42). The resulting libraries were quantified using the Qubit dsDNA BR Assay

460 kit (Invitrogen, catalog no. Q32853), pooled, cleaned using a PCR purification kit, and sequenced
461 on an Illumina MiSeq (PE 2x300). The paired-end reads were assembled using PEAR (43), and
462 reads with more than one expected error were detected using USEARCH (44) and discarded, along
463 with rare sequences (less than 4 reads in a sample). Chimera removal and error correction were
464 performed with the UNOISE3 algorithm (45). Taxonomy was assigned using SINTAX (46) with
465 the RDP training set v18.

466 *16S sequencing data analysis*

467 The following initial analysis steps were performed in Qiime2 (version amplicon-2024.5):
468 Samples were rarefied to 900 reads (based on the histogram of reads per sample), a phylogenetic
469 tree was constructed using MAFFT alignment and FastTree, core alpha and beta diversity metrics
470 were calculated, and principal coordinate analysis (PCoA) matrices were generated. SparCC and
471 Pearson correlation analyses were also performed in Qiime2, using the SCNIC plugin (47). All
472 other analyses were performed in R. PERMANOVA analyses were performed with the adonis2
473 function from the package vegan (version 2.6-10) (48). PERMDISP tests were performed with the
474 permutest function in conjunction with the betadisper function, also from vegan. When testing the
475 effect of time point, permutations were constrained within each enrichment and the data were
476 treated as a series. When testing the effect of field site or sample type, permutations were
477 constrained within time point. Assessment of the contribution of stochastic versus deterministic
478 processes during community assembly was performed using the functions qpen and icamp.big in
479 the iCAMP package (20). Consensus clustering was performed using the package
480 ConsensusClusterPlus, with maxK = 17, reps = 100, pItem = 0.8, pFeature = 1, and clusterAlg =
481 "hc" (49). Except for the consensus clustering plots, which were produced by the
482 ConsensusClusterPlus package, all plots were made with the R package ggplot2 (50).

483 *Scanning electron microscopy*

484 To prepare the scanning electron microscopy (SEM) sample (Electron Microscopy
485 Laboratory, University of California, Berkeley), the Staten Island root 2 10^{-2} enrichment was
486 regrown, from a frozen glycerol stock, in dNMS with 20% methane (shaking at 125 rpm at 25°C).
487 The regrown culture was sub-cultured twice at a 1:100 dilution ratio on day 15 and day 23. On day
488 29, 10 mL of the culture was pelleted (5000 g for 10 min), and the cells were gently resuspended
489 in a fixative solution (2% glutaraldehyde in 0.1M sodium cacodylate buffer, pH 7.2). The sample
490 was placed at 4°C on a rotator overnight and subsequently stored at 4°C in the dark (standing) until
491 further processing. Prior to imaging, the sample was washed 3x in 0.1M sodium cacodylate buffer,
492 pH 7.2, postfixed 3x in 1% osmium tetroxide in 0.1M sodium cacodylate buffer, pH 7.2 for 1 h,
493 and then washed 3x in 0.1M sodium cacodylate buffer, pH 7.2. Samples were dehydrated in a
494 graded ethanol series up to 100%. Samples were then transferred onto 0.1% (w/v) poly-L-lysine–
495 coated coverslips and subjected to critical point drying (Tousimis, Mayland, USA). The dried
496 coverslips were mounted onto aluminum stubs using conductive carbon tape and sputter-coated
497 with a gold/palladium alloy (Safematic GmbH, Switzerland). SEM imaging was performed using
498 a Zeiss Crossbeam 550 (Carl Zeiss Microsystems GmbH, Oberkochen, Germany).

499 *Isolation of strains from the enrichment cultures*

500 Strains were isolated from the original enrichment cultures, as well as enrichments regrown
501 from frozen glycerol stocks, by plating a 10-fold dilution series onto dNMS with 1.5% agarose
502 and 0.2% methanol; dNMS agarose under a mixed methane/air atmosphere; or 0.1x R2A with 1.5%
503 agar. To obtain the *Methylocystis* isolate, a 10-fold dilution series (10^{-1} to 10^{-8}) of an enrichment
504 regrown from the frozen stock was set up in a 48-well plate and incubated statically under 20%
505 methane at room temperature for 4 weeks; then, a loopful of the culture in the 10^{-8} dilution well

506 was streaked onto dNMS agarose and incubated under a mixed methane/air atmosphere. The mixed
507 methane/air atmosphere was achieved by flooding a mostly-closed BD EZ Incubator Container
508 with methane for 30-60s and then quickly latching the lid. All plates were incubated at room
509 temperature, and morphologically distinct colonies were picked and restreaked 3-4 times until the
510 colony morphologies appeared uniform. The 16S rRNA gene was then amplified by colony PCR,
511 using Platinum Hot Start Master Mix (Invitrogen) with the primers 27F
512 (AGAGTTTGATCMTGGCTCAG) and 1492R (TACGGYTACCTTGTTACGACTT). The PCR
513 products were Sanger sequenced at Elim Biopharm, Inc. with the same 27F and 1492R primers.
514 The resulting forward and reverse sequences were aligned in Geneious Prime and subjected to
515 BLAST against the NCBI core nucleotide database.

516 *Genomic analysis of isolated strains*

517 Genomic DNA was isolated from selected strains using the Qiagen DNeasy Blood & Tissue
518 kit (catalog no. 69506), following the manufacturer's protocol for Gram-positive bacteria. Library
519 preparation and whole-genome sequencing was performed by Novogene on an Illumina NovaSeq
520 X Plus. The raw reads were cleaned with Trimmomatic on KBase (51), using the default settings.
521 Draft genomes were assembled with SPAdes (v3.15.3), with the minimum contig size set to 1000
522 bp, and annotated with Prokka (v1.145), also on KBase. Genomes were checked for completeness
523 and contamination with CheckM. Taxonomy was assigned using the Microbial Genomes Atlas
524 pipeline against the Genome Taxonomy Database (GTDB, version r214) (52, 53). Annotation of
525 common carbon source utilization pathways was performed using the online GapMind tool (30).
526 Detection of homologs of known methanol dehydrogenases was performed using DIAMOND with
527 the "sensitive" setting [REF]; a hit was considered a homolog if it had >40% identity to the
528 reference sequence, with at least 80% coverage. The list of reference methanol dehydrogenase

529 sequences was obtained from a prior publication (54). For C1 assimilation pathways, DIAMOND
530 with the same settings failed to detect complete pathways in some of the known methylotrophs.
531 We therefore instead used HMMER (version 3.4) (55) with the HMM profiles from the same prior
532 publication (54), requiring hits to have at least 80% coverage of the respective model to be
533 considered a homolog.

534 *Data availability*

535 All data is available from the authors upon reasonable request.

536 **References**

537 1. Hanson RS, Hanson TE. 1996. Methanotrophic bacteria. Microbiol Rev 60:439–471.

538 2. Auman AJ, Speake CC, Lidstrom ME. 2001. nifH Sequences and Nitrogen Fixation in Type
539 I and Type II Methanotrophs. Appl Environ Microbiol 67:4009–4016.

540 3. Eisentraeger A, Klag P, Vansbotter B, Heymann E, Dott W. 2001. Denitrification of
541 groundwater with methane as sole hydrogen donor. Water Research 35:2261–2267.

542 4. Knowles R. 2005. Denitrifiers associated with methanotrophs and their potential impact on
543 the nitrogen cycle. Ecological Engineering 24:441–446.

544 5. Chistoserdova L, Kalyuzhnaya MG. 2018. Current Trends in Methylotrophy. Trends in
545 Microbiology 26:703–714.

546 6. Whittenbury R, Phillips KC, Wilkinson JF. 1970. Enrichment, Isolation and Some Properties
547 of Methane-utilizing Bacteria. Journal of General Microbiology 61:205–218.

548 7. Ho A, De Roy K, Thas O, De Neve J, Hoefman S, Vandamme P, Heylen K, Boon N. 2014.
549 The more, the merrier: heterotroph richness stimulates methanotrophic activity. The ISME
550 Journal 8:1945–1948.

551 8. Stock M, Hoefman S, Kerckhof F-M, Boon N, De Vos P, De Baets B, Heylen K, Waegeman
552 W. 2013. Exploration and prediction of interactions between methanotrophs and heterotrophs.
553 Research in Microbiology 164:1045–1054.

554 9. Iguchi H, Yurimoto H, Sakai Y. 2011. Stimulation of Methanotrophic Growth in Cocultures
555 by Cobalamin Excreted by Rhizobia. Appl Environ Microbiol 77:8509–8515.

556 10. Qiu Q, Conrad R, Lu Y. 2009. Cross-feeding of methane carbon among bacteria on rice roots
557 revealed by DNA-stable isotope probing. Environ Microbiol Rep 1:355–361.

558 11. Murase J, Frenzel P. 2007. A methane-driven microbial food web in a wetland rice soil.
559 Environmental Microbiology 9:3025–3034.
560 12. Chen K-H, Feng J, Bodelier PLE, Yang Z, Huang Q, Delgado-Baquerizo M, Cai P, Tan W,
561 Liu Y-R. 2024. Metabolic coupling between soil aerobic methanotrophs and denitrifiers in
562 rice paddy fields. Nat Commun 15:3471.
563 13. Osaka T, Ebie Y, Tsuneda S, Inamori Y. 2008. Identification of the bacterial community
564 involved in methane-dependent denitrification in activated sludge using DNA stable-isotope
565 probing: Characterization of a MDD ecosystem by SIP. FEMS Microbiology Ecology
566 64:494–506.
567 14. Dumont MG, Pommerenke B, Casper P, Conrad R. 2011. DNA-, rRNA- and mRNA-based
568 stable isotope probing of aerobic methanotrophs in lake sediment. Environmental
569 Microbiology 13:1153–1167.
570 15. Hutchens E, Radajewski S, Dumont MG, McDonald IR, Murrell JC. 2004. Analysis of
571 methanotrophic bacteria in Movile Cave by stable isotope probing. Environmental
572 Microbiology 6:111–120.
573 16. Bridgham SD, Cadillo-Quiroz H, Keller JK, Zhuang Q. 2013. Methane emissions from
574 wetlands: biogeochemical, microbial, and modeling perspectives from local to global scales.
575 Global Change Biology 19:1325–1346.
576 17. Cao W, Cai Y, Bao Z, Wang S, Yan X, Jia Z. 2022. Methanotrophy Alleviates Nitrogen
577 Constraint of Carbon Turnover by Rice Root-Associated Microbiomes. Front Microbiol
578 13:885087.

579 18. Muthayya S, Sugimoto JD, Montgomery S, Maberly GF. 2014. An overview of global rice
580 production, supply, trade, and consumption. Annals of the New York Academy of Sciences
581 1324:7–14.
582 19. Neufeld JD, Dumont MG, Vohra J, Murrell JC. 2007. Methodological Considerations for the
583 Use of Stable Isotope Probing in Microbial Ecology. Microbial Ecology 53:435–442.
584 20. Ning D, Yuan M, Wu L, Zhang Y, Guo X, Zhou X, Yang Y, Arkin AP, Firestone MK, Zhou J.
585 2020. A quantitative framework reveals ecological drivers of grassland microbial community
586 assembly in response to warming. Nat Commun 11:4717.
587 21. Stegen JC, Lin X, Fredrickson JK, Chen X, Kennedy DW, Murray CJ, Rockhold ML,
588 Konopka A. 2013. Quantifying community assembly processes and identifying features that
589 impose them. The ISME Journal 7:2069–2079.
590 22. Stegen JC, Lin X, Fredrickson JK, Konopka AE. 2015. Estimating and mapping ecological
591 processes influencing microbial community assembly. Front Microbiol 6:370.
592 23. Monti S, Tamayo P, Mesirov J, Golub T. 2003. Consensus Clustering: A Resampling-Based
593 Method for Class Discovery and Visualization of Gene Expression Microarray Data. Machine
594 Learning 52:91–118.
595 24. Celiker H, Gore J. 2014. Clustering in community structure across replicate ecosystems
596 following a long-term bacterial evolution experiment. Nat Commun 5:4643.
597 25. Méheust R, Burstein D, Castelle CJ, Banfield JF. 2019. The distinction of CPR bacteria from
598 other bacteria based on protein family content. Nat Commun 10:4173.
599 26. Ji Y, Zhang P, Zhou S, Gao P, Wang B, Jiang J. 2022. Widespread but Poorly Understood
600 Bacteria: Candidate Phyla Radiation. Microorganisms 10:2232.

601 27. Friedman J, Alm EJ. 2012. Inferring Correlation Networks from Genomic Survey Data.
602 PLOS Computational Biology 8:e1002687.
603 28. Weiss S, Van Treuren W, Lozupone C, Faust K, Friedman J, Deng Y, Xia LC, Xu ZZ, Ursell
604 L, Alm EJ, Birmingham A, Cram JA, Fuhrman JA, Raes J, Sun F, Zhou J, Knight R. 2016.
605 Correlation detection strategies in microbial data sets vary widely in sensitivity and precision.
606 ISME J 10:1669–1681.
607 29. Krause SMB, Johnson T, Samadhi Karunaratne Y, Fu Y, Beck DAC, Chistoserdova L,
608 Lidstrom ME. 2017. Lanthanide-dependent cross-feeding of methane-derived carbon is
609 linked by microbial community interactions. Proc Natl Acad Sci USA 114:358–363.
610 30. Price MN, Deutschbauer AM, Arkin AP. 2022. Filling gaps in bacterial catabolic pathways
611 with computation and high-throughput genetics. PLoS Genet 18:e1010156.
612 31. Chistoserdova L. 2011. Modularity of methylotrophy, revisited. Environmental Microbiology
613 13:2603–2622.
614 32. Oshkin IY, Beck DAC, Lamb AE, Tchesnokova V, Benuska G, McTaggart TL, Kalyuzhnaya
615 MG, Dedysh SN, Lidstrom ME, Chistoserdova L. 2015. Methane-fed microbial microcosms
616 show differential community dynamics and pinpoint taxa involved in communal response.
617 The ISME Journal 9:1119–1129.
618 33. Van Grinsven S, Sinninghe Damsté JS, Harrison J, Polerecky L, Villanueva L. 2021. Nitrate
619 promotes the transfer of methane-derived carbon from the methanotroph *Methylobacter* sp.
620 to the methylotroph *Methylotenera* sp. in eutrophic lake water. Limnology & Oceanography
621 66:878–891.
622 34. Karwautz C, Kus G, Stöckl M, Neu TR, Lueders T. 2018. Microbial megacities fueled by
623 methane oxidation in a mineral spring cave. The ISME Journal 12:87–100.

624 35. Brown CT, Hug LA, Thomas BC, Sharon I, Castelle CJ, Singh A, Wilkins MJ, Wrighton KC,
625 Williams KH, Banfield JF. 2015. Unusual biology across a group comprising more than 15%
626 of domain Bacteria. Nature 523:208–211.
627 36. Vecherskaya M, Dijkema C, Saad HR, Stams AJM. 2009. Microaerobic and anaerobic
628 metabolism of a Methylocystis parvus strain isolated from a denitrifying bioreactor.
629 Environmental Microbiology Reports 1:442–449.
630 37. Tays C, Guarnieri MT, Sauvageau D, Stein LY. 2018. Combined effects of carbon and
631 nitrogen source to optimize growth of proteobacterial methanotrophs. Front Microbiol 9:2239.
632 38. Kalyuzhnaya MG, Yang S, Rozova ON, Smalley NE, Clubb J, Lamb A, Gowda GAN, Raftery
633 D, Fu Y, Bringel F, Vuilleumier S, Beck DAC, Trotsenko YA, Khmelenina VN, Lidstrom ME.
634 2013. Highly efficient methane biocatalysis revealed in a methanotrophic bacterium. Nat
635 Commun 4:2785.
636 39. Gavriilidou A, Gutleben J, Versluis D, Forgiarini F, van Passel MWJ, Ingham CJ, Smidt H,
637 Sipkema D. 2020. Comparative genomic analysis of Flavobacteriaceae: insights into
638 carbohydrate metabolism, gliding motility and secondary metabolite biosynthesis. BMC
639 Genomics 21:569.
640 40. Rahalkar MC, Khatri K, Pandit P, Bahulikar RA, Mohite JA. 2021. Cultivation of Important
641 Methanotrophs From Indian Rice Fields. Front Microbiol 12:669244.
642 41. Thompson LR, Sanders JG, McDonald D, Amir A, Ladau J, Locey KJ, Prill RJ, Tripathi A,
643 Gibbons SM, Ackermann G, Navas-Molina JA, Janssen S, Kopylova E, Vázquez-Baeza Y,
644 González A, Morton JT, Mirarab S, Zech Xu Z, Jiang L, Haroon MF, Kanbar J, Zhu Q, Jin
645 Song S, Kosciolek T, Bokulich NA, Lefler J, Brislawn CJ, Humphrey G, Owens SM,
646 Hampton-Marcell J, Berg-Lyons D, McKenzie V, Fierer N, Fuhrman JA, Clauset A, Stevens

647 RL, Shade A, Pollard KS, Goodwin KD, Jansson JK, Gilbert JA, Knight R. 2017. A
648 communal catalogue reveals Earth's multiscale microbial diversity. Nature 551:457–463.
649 42. Lundberg DS, Yourstone S, Mieczkowski P, Jones CD, Dangl JL. 2013. Practical innovations
650 for high-throughput amplicon sequencing. Nat Methods 10:999–1002.
651 43. Zhang J, Kobert K, Flouri T, Stamatakis A. 2014. PEAR: a fast and accurate Illumina Paired-
652 End reAd mergeR. Bioinformatics 30:614–620.
653 44. Edgar RC. Search and clustering orders of magnitude faster than BLAST.
654 45. Edgar RC. 2016. UNOISE2: improved error-correction for Illumina 16S and ITS amplicon
655 sequencing. bioRxiv https://doi.org/10.1101/081257.
656 46. Edgar RC. 2016. SINTAX: a simple non-Bayesian taxonomy classifier for 16S and ITS
657 sequences. bioRxiv https://doi.org/10.1101/074161.
658 47. Shaffer M, Thurimella K, Sterrett JD, Lozupone CA. 2023. SCNIC: Sparse correlation
659 network investigation for compositional data. Molecular Ecology Resources 23:312–325.
660 48. Oksanen J, Simpson GL, Blanchet FG, Kindt R, Legendre P, Minchin PR, O'Hara RB,
661 Solymos P, Stevens MHH, Szoecs E, Wagner H, Barbour M, Bedward M, Bolker B, Borcard
662 D, Borman T, Carvalho G, Chirico M, Caceres MD, Durand S, Evangelista HBA, FitzJohn
663 R, Friendly M, Furneaux B, Hannigan G, Hill MO, Lahti L, Martino C, McGlinn D, Ouellette
664 M-H, Cunha ER, Smith T, Stier A, Braak CJFT, Weedon J. 2025. vegan: Community Ecology
665 Package (2.6-10).
666 49. Wilkerson MD, Hayes DN. 2010. ConsensusClusterPlus: a class discovery tool with
667 confidence assessments and item tracking. Bioinformatics 26:1572–1573.
668 50. Wickham H. 2016. ggplot2: Elegant Graphics for Data Analysis. Springer-Verlag New York.
669 https://ggplot2.tidyverse.org.

670 51. Arkin AP, Cottingham RW, Henry CS, Harris NL, Stevens RL, Maslov S, Dehal P, Ware D,
671 Perez F, Canon S, Sneddon MW, Henderson ML, Riehl WJ, Murphy-Olson D, Chan SY,
672 Kamimura RT, Kumari S, Drake MM, Brettin TS, Glass EM, Chivian D, Gunter D, Weston
673 DJ, Allen BH, Baumohl J, Best AA, Bowen B, Brenner SE, Bun CC, Chandonia J-M, Chia
674 J-M, Colasanti R, Conrad N, Davis JJ, Davison BH, DeJongh M, Devoid S, Dietrich E,
675 Dubchak I, Edirisinghe JN, Fang G, Faria JP, Frybarger PM, Gerlach W, Gerstein M, Greiner
676 A, Gurtowski J, Haun HL, He F, Jain R, Joachimiak MP, Keegan KP, Kondo S, Kumar V,
677 Land ML, Meyer F, Mills M, Novichkov PS, Oh T, Olsen GJ, Olson R, Parrello B, Pasternak
678 S, Pearson E, Poon SS, Price GA, Ramakrishnan S, Ranjan P, Ronald PC, Schatz MC, Seaver
679 SMD, Shukla M, Sutormin RA, Syed MH, Thomason J, Tintle NL, Wang D, Xia F, Yoo H,
680 Yoo S, Yu D. 2018. KBase: The United States Department of Energy Systems Biology
681 Knowledgebase. Nat Biotechnol 36:566–569.
682 52. Parks DH, Chuvochina M, Rinke C, Mussig AJ, Chaumeil P-A, Hugenholtz P. GTDB: an
683 ongoing census of bacterial and archaeal diversity through a phylogenetically consistent, rank
684 normalized and complete genome-based taxonomy.
685 53. Rodriguez-R LM, Gunturu S, Harvey WT, Rosselló-Mora R, Tiedje JM, Cole JR,
686 Konstantinidis KT. 2018. The Microbial Genomes Atlas (MiGA) webserver: taxonomic and
687 gene diversity analysis of Archaea and Bacteria at the whole genome level. Nucleic Acids
688 Res 46:W282–W288.
689 54. Salcher MM, Schaefle D, Kaspar M, Neuenschwander SM, Ghai R. 2019. Evolution in action:
690 habitat transition from sediment to the pelagial leads to genome streamlining in
691 Methylophilaceae. ISME J 13:2764–2777.

692 55. Eddy SR. 2011. Accelerated Profile HMM Searches. PLOS Computational Biology
693 7:e1002195.
694
695

Figures and Figure Legends

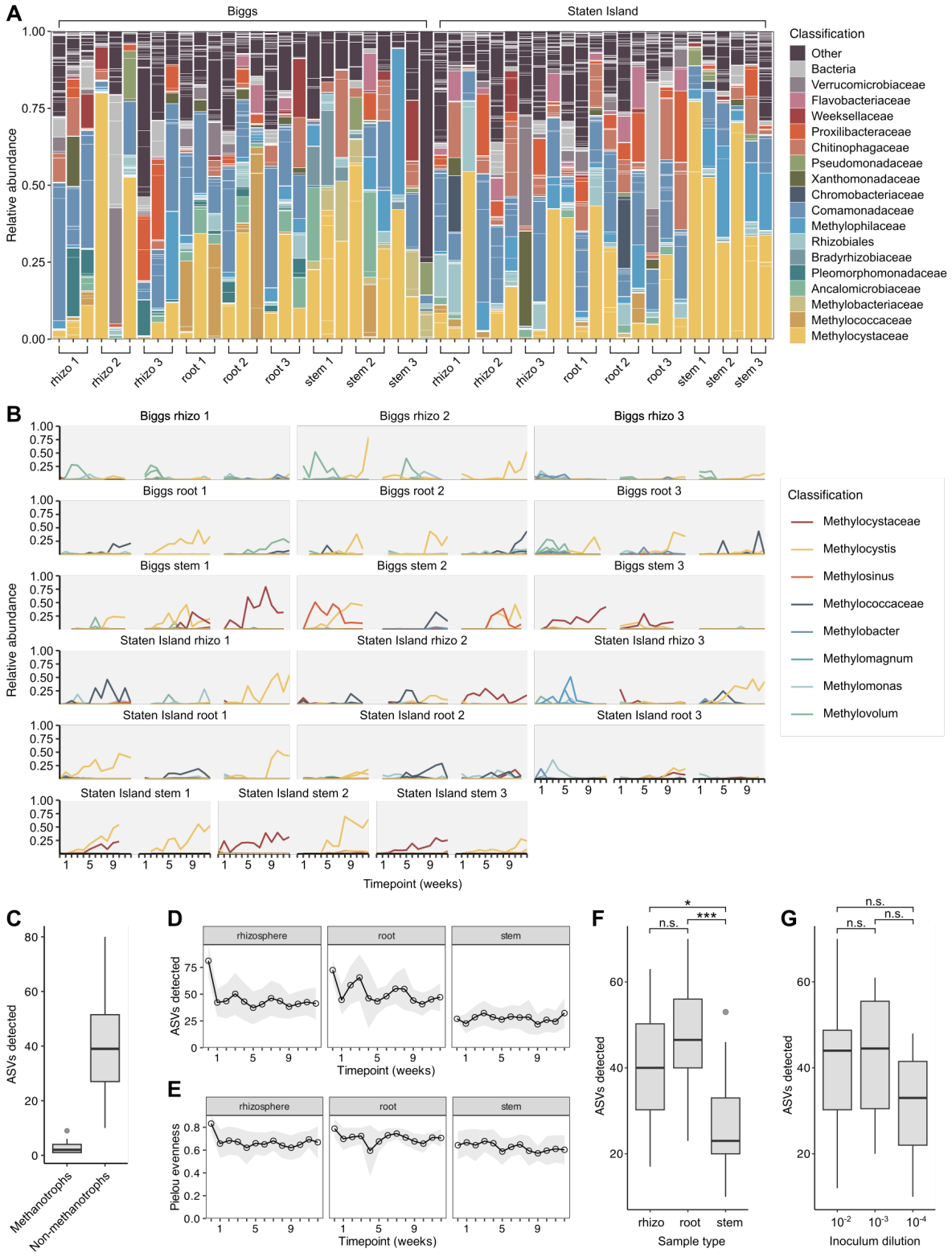

698 **Figure 1. Taxonomic diversity and dynamics of methane-fed enrichment cultures. A)** Taxa
699 bar plot showing the overall diversity and major families in the enrichment cultures at the final
700 sequenced timepoint. Individual ASVs within each family are separated by white lines. **B)** Relative
701 abundance of putative methanotroph ASVs over time in each enrichment. Under each header (e.g.
702 "Biggs rhizo 1"), the enrichments are arranged from left to right in order of increasing inoculum
703 dilution (i.e., 10^{-2}, 10^{-3}, 10^{-4}). **C)** The number of detected ASVs that were classified as
704 methanotrophs or non-methanotrophs in each enrichment at the final timepoint. **D-E)** The number
705 of ASVs detected (D) or Pielou evenness (E) of the enrichments over time, separated by sample
706 type. **F)** The number of ASVs detected in the enrichments at the final timepoint, separated by
707 sample type or by inoculum dilution. * $p < 0.05$, *** $p < 0.001$, ANOVA followed by Tukey HSD.

708

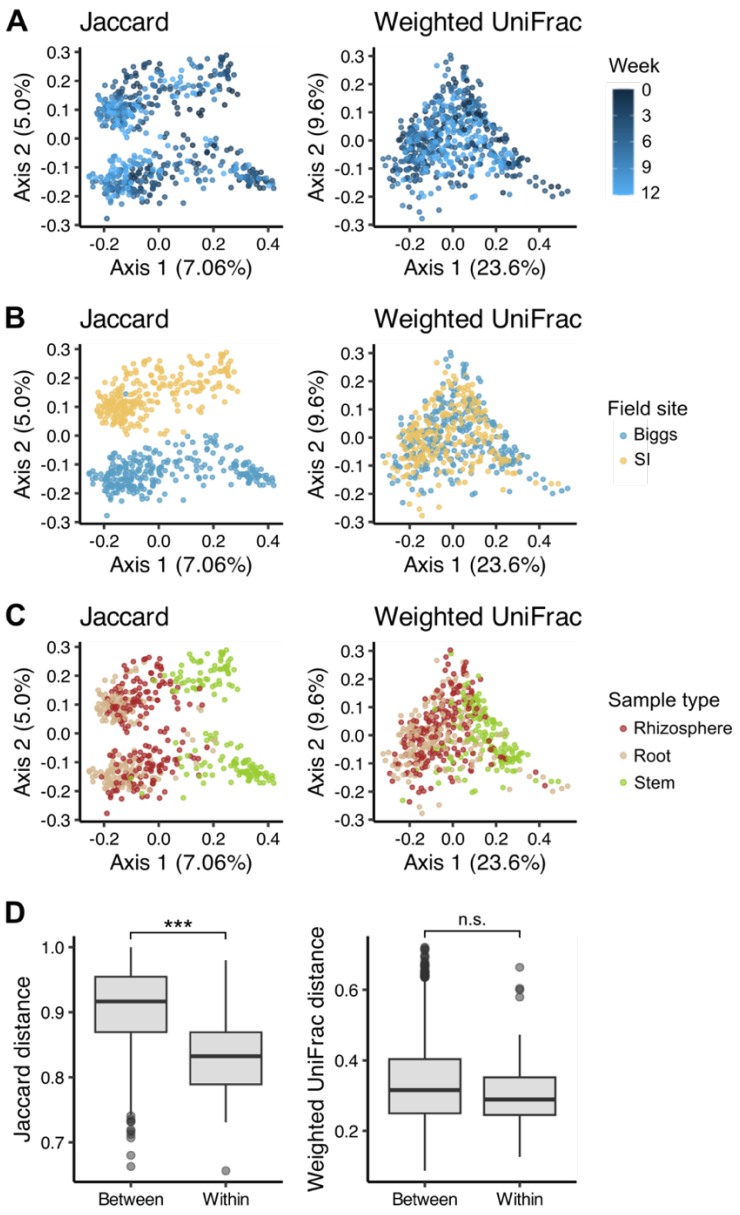

Figure 2. Impact of external variables on enrichment community beta diversity. A) PCoA plots of all sequenced enrichment samples, colored by time point. **B)** The same plots as in (A), but colored by field site. **C)** The same plots as in (A), but colored by sample type. **D)** Jaccard and weighted UniFrac distances for enrichments inoculated from different replicate plant parts ("between") versus enrichments inoculated from the same replicate plant part (albeit at different dilutions; "within").

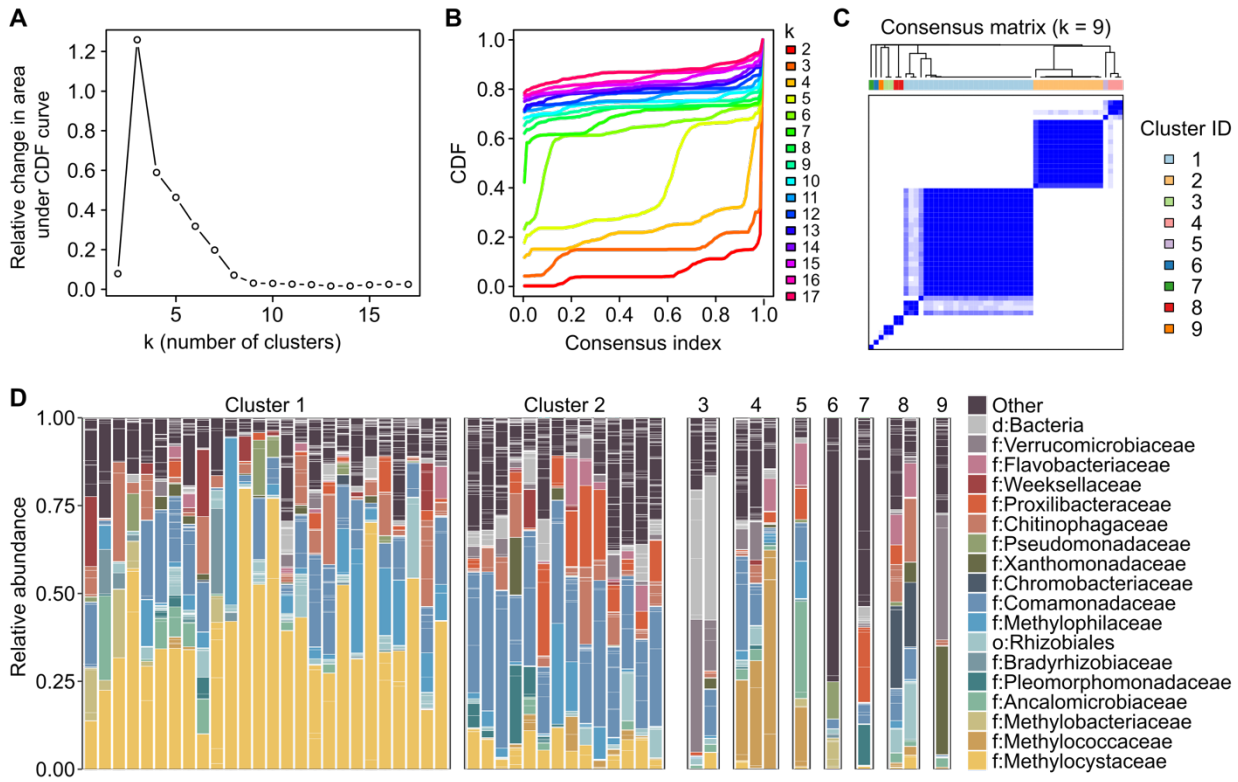

Figure 3. Consensus clustering analysis of enrichment communities. A) Delta area plot showing the relative change in area under the cumulative distribution function (CDF) curve for k versus $k - 1$. The optimal number of clusters is usually considered to be the value of k at which there is no longer an appreciable increase in area under the CDF. **B)** The CDFs of the consensus matrix for each k (indicated by colors), estimated by a histogram of 100 bins. **C)** The consensus matrix for $k = 9$. Darker blues in the matrix indicate higher consensus. **D)** Taxa bar plots for the samples in each consensus cluster for $k = 9$.

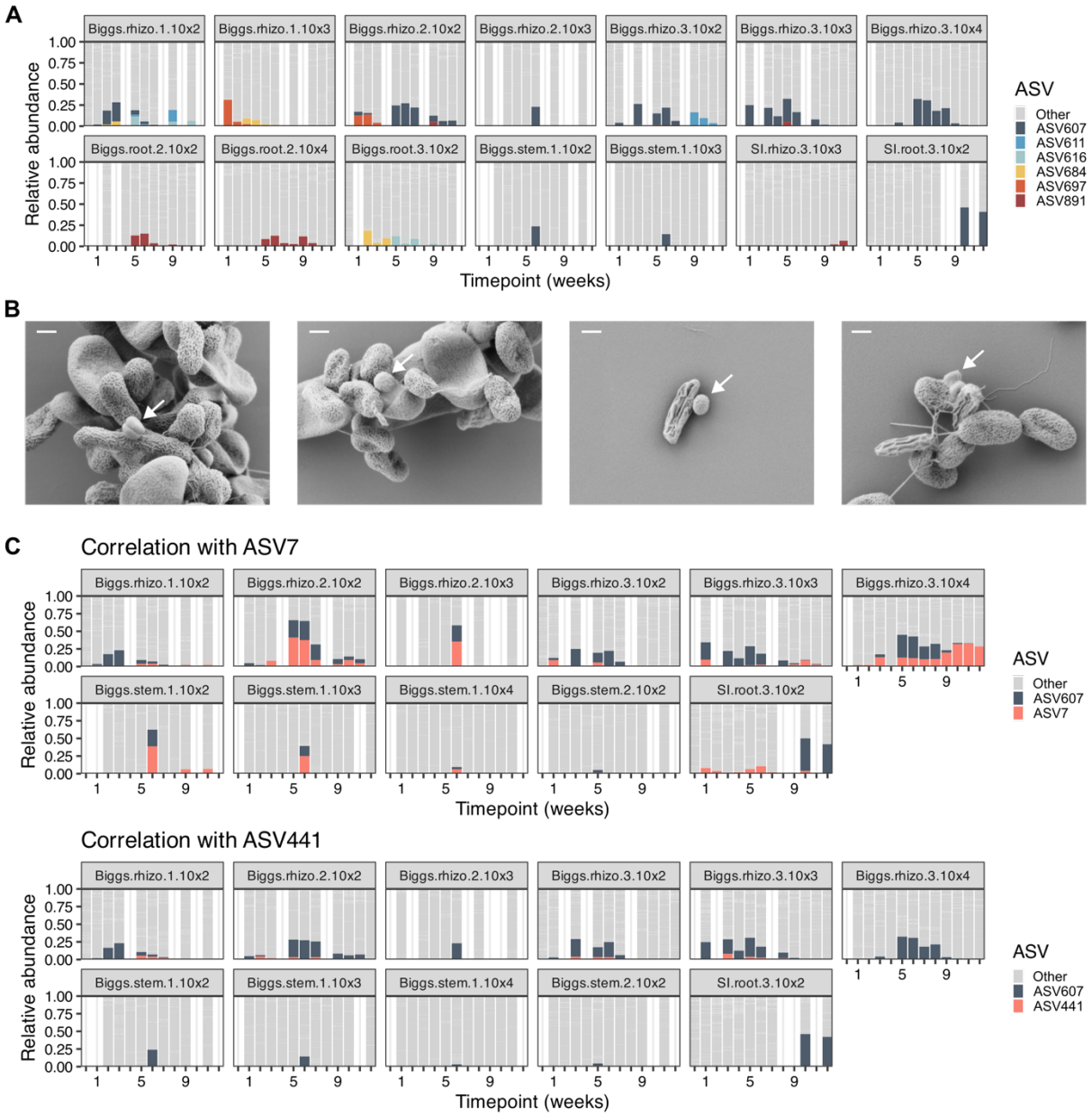

Figure 4. Presence of CPR bacteria in methane-fed enrichments. A) Taxa bar plot highlighting the six unclassified bacterial ASVs that appeared at a relative abundance of >5% at least three times (whether in different enrichments or multiple timepoints of a single enrichment). **B)** SEM images showing the putative CPR epibiont, marked with a white arrow. Scale bar = 300 nm. **C)** Taxa bar plots highlighting ASV607 along with the two candidates for its host based on correlation analysis.

Figure 5. Putative carbon source utilization pathways in non-methanotrophic isolates from methane-fed enrichments. The completeness of pathways for utilizing 62 common carbon sources was assessed using GapMind. "Complete" indicates that a complete pathway was found with only high-confidence steps; "Maybe" indicates that the pathway was found but at least one step was at best medium-confidence; "Gap" indicates that one or more steps was missing or low-confidence.

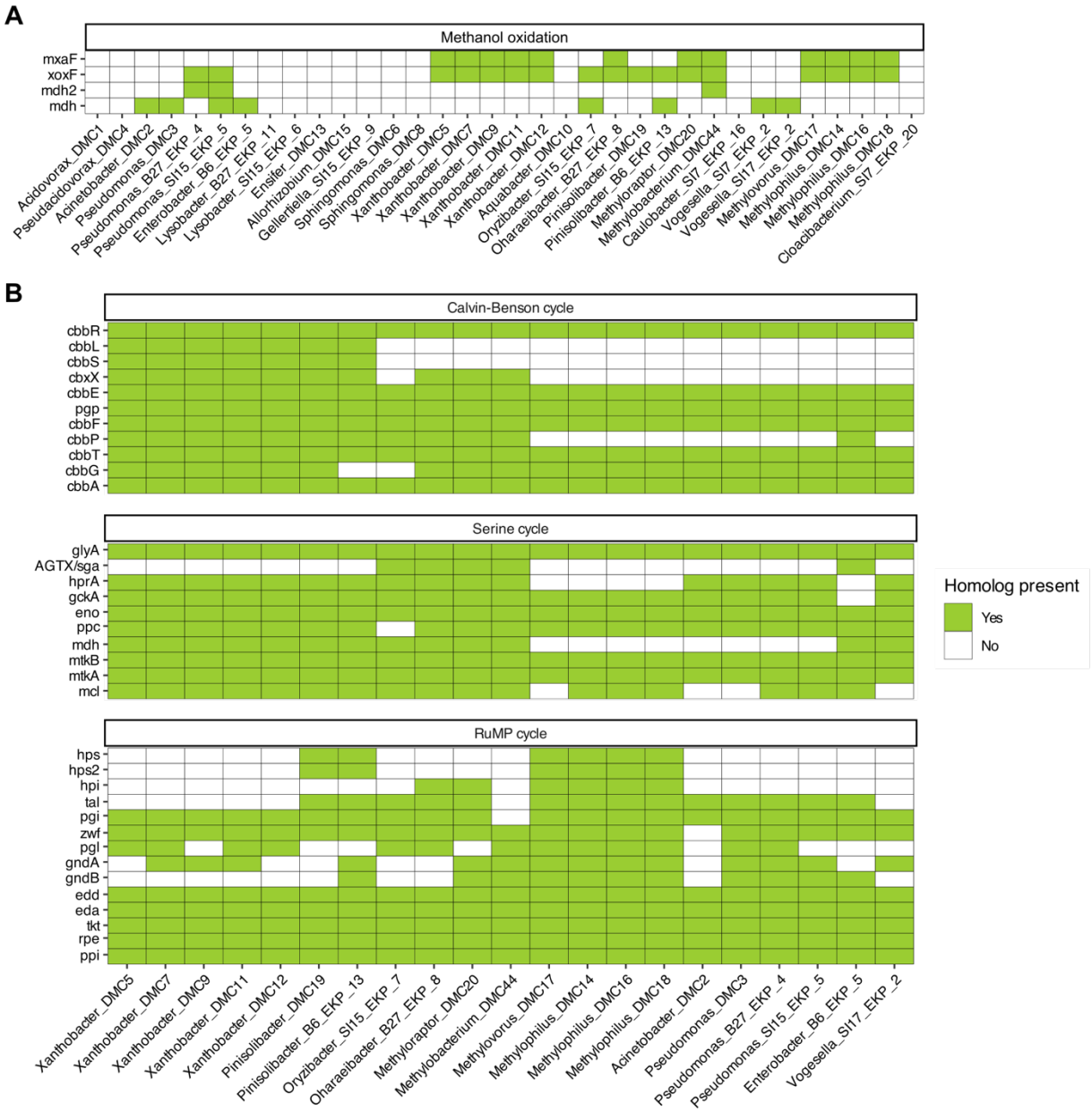

Figure 6. Genomic capacity for methanol catabolism in non-methanotrophic isolates from methane-fed enrichments. A) Presence of homologs of known methanol dehydrogenases in all of the sequenced non-methanotrophic isolates. Green = present, white = absent. **B)** Presence of the genes needed for the three known bacterial C1 assimilation pathways in strains possessing at least one putative methanol dehydrogenase.

747 **Table 1. PERMANOVA and PERMDISP statistical test results.**

Distance metric	Test	Independent variable	R^2	Pseudo-F	Pr(>F)
Jaccard	PERMANOVA	Timepoint	0.04	2.0427	0.001
Weighted UniFrac	PERMANOVA	Timepoint	0.08	3.8124	0.001
Jaccard	PERMDISP	Timepoint	NA	5.8664	0.001
Weighted UniFrac	PERMDISP	Timepoint	NA	8.0389	0.001
Jaccard	PERMANOVA	Field site	0.05	25.623	0.001
Weighted UniFrac	PERMANOVA	Field site	0.03	14.035	0.001
Jaccard	PERMDISP	Field site	NA	50.335	0.001
Weighted UniFrac	PERMDISP	Field site	NA	19.947	0.001
Jaccard	PERMANOVA	Sample type	0.07	20.108	0.001
Weighted UniFrac	PERMANOVA	Sample type	0.13	39.414	0.001
Jaccard	PERMDISP	Sample type	NA	51.113	0.001
Weighted UniFrac	PERMDISP	Sample type	NA	17.582	0.001
Jaccard	PERMANOVA	Enrichment ID	0.52	10.412	0.001
Weighted UniFrac	PERMANOVA	Enrichment ID	0.44	7.4642	0.001
Jaccard	PERMANOVA	Replicate (marginal effect*)	0.01	7.9084	0.001
Weighted UniFrac	PERMANOVA	Replicate (marginal effect*)	0.01	7.9996	0.001
Jaccard	PERMANOVA	Dilution (marginal effect*)	0.02	6.1119	0.001
Weighted UniFrac	PERMANOVA	Dilution (marginal effect*)	0.02	7.8126	0.001

748 *Marginal effect indicates the effect of the term after taking into account all other terms in the

749 model (the terms were timepoint, field site, sample type, replicate, and dilution).

750